Geoderma 395 (2021) 115080

Contents lists available at ScienceDirect

Geoderma

journal homepage: www.elsevier.com/locate/geoderma

Distribution and chemical species of phosphorus across density fractions in Andisols of contrasting mineralogy

Akira Takamoto [a,b], Yohey Hashimoto [a,*], Maki Asano [c], Keiichi Noguchi [d], Rota Wagai [e]

[a] Department of Bio-Applications and Systems Engineering, Tokyo University of Agriculture and Technology, Koganei, Tokyo, 184-8588, Japan
[b] Daisen Research Station, Tohoku Agricultural Research Center, NARO, Daisen, Akita, 014-0102, Japan
[c] Faculty of Life and Environmental Sciences, University of Tsukuba, Tsukuba, Ibaraki, 305-8572, Japan
[d] Instrumentation Analysis Center, Tokyo University of Agriculture and Technology, Koganei, Tokyo, 184-8588, Japan
[e] Institute for Agro-Environmental Sciences, NARO, Tsukuba, Ibaraki, 305-8604, Japan

ARTICLE INFO

Handling Editor: Jan Willem Van Groenigen

Keywords:
Phosphate
Andosols
Sequential extraction
Volcanic ash soils
Hedley
XAFS
NMR

ABSTRACT

Strong control of iron (Fe) and aluminum (Al) phases on soil phosphorus (P) dynamics is well established. How organic and inorganic P forms are associated with Fe and Al phases remains poorly understood, and sequential density fractionation thus allows one to assess the soil continuum from organic-rich particles (< 1.8 g cm^{-3}) to organo-mineral particles (1.8–2.25 g cm^{-3}), and finally to mineral rich particles (> 2.25 g cm^{-3}). We combined the density fractionation approach with wet extraction techniques, ^{31}P NMR spectroscopy and X-ray absorption near-edge structure (XANES) spectroscopy to investigate the distribution and chemical species of P in relation to Fe and Al phases for two Andisols: an allophanic Andisol rich in short-range-order aluminosilicates (silandic) and a non-allophanic Andisol rich in organic matter (OM) and organo-aluminum complexes (aluandic). We fractionated the soils to the density classes of 1.6–1.8, 1.8–2.0, 2.0–2.25, 2.25–2.5, and > 2.5 g cm^{-3} using the sodium polytungstate solutions. Across five density fractions, inorganic and total P were distributed in low to *meso*-density fractions (1.6–2.25 g cm^{-3}) where major portions of extractable Fe and Al were found. The major P pool was found in the NaOH extraction step for low- to *meso*-density ranges (< 2.25 g cm^{-3}), suggesting that Al and Fe (oxyhydr)oxides and aluminosilicates have significant roles in P sorption in allophanic and non-allophanic Andisols. In contrast, the residual P remaining after the sequential extraction was predominant in heavier-density fractions (> 2.25 g cm^{-3}). Molybdate-reactive and total P extracted by NaOH in the density fractions were positively correlated with oxalate extractable Al (Al_{ox}) in the allophanic Andisol ($r > 0.91$) and with pyrophosphate extractable Al (Al_p) in the non-allophanic Andisol ($r > 0.97$), suggesting stronger control of Al phases to P over Fe phases. The non-destructive XANES analysis confirmed that P in both Andisols was associated primarily with Al, not Fe, and suggested the presence of P bound to organo-Al complexes in the non-allophanic Andisol (up to 76% of P in the 1.6–1.8 g cm^{-3} fraction where Al_p is enriched). Solution ^{31}P NMR spectra of NaOH-EDTA soil extracts showed that the primary organic P group was phosphomonoesters that decreased with increasing density in allophanic and non-allophanic Andisols. *Myo*-inositol hexakisphosphate (IHP) and *scyllo*-IHP were identified in a density fraction between 1.8 and 2.25 g cm^{-3} of non-allophanic Andisol. Our study highlights the importance of low- to *meso*-density fractions in organic and inorganic P reservoirs in Andisols.

1. Introduction

High phosphorus (P) retention capacity is a unique property of Andisols, setting a major agronomic challenge in volcanic regions of the world. Andisols are classified into two groups, namely allophanic and non-allophanic Andisols, based on the predominant clay minerals (Shoji et al., 1993). Allophanic Andisols (silandic Andosol in WRB classification) are characterized by the dominance of allophane, imogolite, and proto-imogolite type minerals. In comparison, non-allophanic Andisols (aluandic) have lower pH, higher contents of organic matter (OM), organo-Al/Fe complexes, and 2:1 phyllosilicates (Shoji et al., 1993). The short-range-order Al/Fe phases and organo-Al/Fe complexes contribute to P sorption capacity of allophanic and non-allophanic Andisols, respectively (Hashimoto et al., 2012). Statistically

* Corresponding author.

https://doi.org/10.1016/j.geoderma.2021.115080
Received 7 July 2020; Received in revised form 23 December 2020; Accepted 5 March 2021
Available online 26 March 2021

and experimentally, P sorption capacity of allophanic and non-allophanic Andisols was associated directly with oxalate-extractable Al (Al_{ox}) and pyrophosphate-extractable Al (Al_p), respectively (Gunjigake and Wada, 1981; Hashimoto et al., 2012). However, current knowledge of P studies in Andisols is limited to inorganic P from macroscopic viewpoints (e.g., extraction and adsorption isotherm), and the differences in P fractionation along soil density gradients remain unclear between allophanic and non-allophanic Andisols.

An effective approach to examine P accumulation and its linkage with soil organic and inorganic components is to sort them by density. The density of soil particles is determined by two factors; one is the absolute density of individual organic and mineral particles, and the other is the relative amounts of organic and mineral matter in the particle as soil particles are largely present as organo-mineral particles or aggregates (Sollins et al., 1999; Turchenek and Oades, 1979; Wagai et al., 2020). In general, the absolute density of minerals ranges 2.3–2.8 g cm^{-3} in which allophane and imogolite are around 2.7–2.8 g cm^{-3} (Wada and Wada, 1977) and iron minerals can be 3.8–5.3 g cm^{-3} (Cornell and Schwertmann, 2006). On the other hand, the density of soil OM is much lower, typically 1.3–1.6 g cm^{-3} (Kaiser and Guggenberger, 2007; Mayer et al., 2004). Both individual minerals and organo-Al complexes play important roles in soil P sorption (e.g., Hashimoto et al., 2012), attesting to the advantage of density fractionation approach to study processes of soil P accumulation and distribution. The use of density fractionation method together with elemental analysis and P speciation contributes to elucidating the mechanisms and processes of P accumulation in soils.

Little has been reported on soil P using density fractionation techniques (Pierzynski et al., 1990; Six et al., 2001). Pierzynski et al. (1990) separated soil's clay fractions into < 2.2, 2.2–2.5, and > 2.5 g cm^{-3} and found that total P distributed more in the < 2.2 g cm^{-3} fraction than in the other fractions. Six et al. (2001) using ^{1}H and ^{31}P nuclear magnetic resonance (NMR) showed that aliphatic hydrocarbons and phosphomonoesters were major species in the density fraction between 2.0 and 2.2 g cm^{-3} of fine-silt particles (2–20 μm). In comparison, the density fractionation approach has been frequently used to characterize soil OM (Sollins et al., 2009, 2006). From low- to high-density fractions, a wide range of soils have shown a progressive decline in total C and N, C/N ratio, and lignin contents and concurrent increases in the degree of microbial processing of OM (enrichment in $\delta^{13}C$ and $\delta^{15}N$) and in ^{14}C-based stability of OM (Baisden et al., 2002; Crow et al., 2015; Jones and Singh, 2014; Sollins et al., 2009, 2006; Wagai et al., 2018). Biogeochemical reactions of C and N are closely associated with P in soils (Hou et al., 2012; Mori et al., 2017; Wang et al., 2010). Thus, characterization of soil P along soil particle density gradients would be a promising approach to better understand soil P cycling.

This study aimed to examine the distribution and chemical species of P and its association with the metals (Al and Fe) extracted by pyrophosphate and acid oxalate solutions across five density fractions separated from allophanic and non-allophanic Andisols. To achieve this, we used sequential P extraction, P K-edge X-ray absorption near-edge structure (XANES) spectroscopy, and solution ^{31}P NMR spectroscopy for the density fractions relatively high in P concentrations. Short-range-order Al/Fe phases and organo-Al/Fe complexes were considered to be important for P sorption in allophanic and non-allophanic Andisols, respectively (Gunjigake and Wada, 1981; Hashimoto et al., 2012; Hiradate and Uchida, 2004). We thus expected that the contrasting mineralogy and soil colloids between the allophanic and non-allophanic Andisols would allow us to identify the role of specific metal phases for the distribution and accumulation of soil P species along the density gradients.

2. Material and method

2.1. Soil characterization

An allophanic Andisol sample (hereafter Tsukuba soil) was collected from the experimental field at Institute for Agro-Environmental Sciences, NARO in Tsukuba, Japan (36°01′N, 140°07′E, 21 m above sea level). The field has been cultivated with soybean/winter-wheat rotation under conventional tillage since the year 1983. The allophanic Andisols was classified as Hydric Hapludand (Soil Taxonomy) and Hydric-Silic Andosol (World Reference Base for Soil Resources). The soil was sampled from the entire plow layer (0–20 cm). A non-allophanic Andisol sample (hereafter Kawatabi soil) was collected from Kawatabi Field Science at Tohoku University, Japan (38°44′N, 140°45′E, 190 m above mean sea level). The soil was sampled in the Ap horizon (0–16 cm) after harvest of potato and classified as Alic Hapludand (Soil Taxonomy) and Melanic Aluandic Andosol (World Reference Base for Soil Resources). These soils are representative of allophanic and non-allophanic Andisols in Japan and well-characterized from physical, chemical, and agronomic standpoints (Asano and Wagai, 2014; Saigusa et al., 1994; Shoji and Fujiwara, 1984; Wagai et al., 2013). Further information on the sampling site of allophanic and non-allophanic Andisols was described in detail by Wagai et al. (2018) and Ito and Saigusa (1996), respectively. The allophanic Andisols sample used in this study was the same as reported by Asano and Wagai (2014). The collected soils were air-dried and then passed through a 2 mm sieve. The basic soil chemical and mineralogical properties of the soils were determined by the standard procedures (Sparks et al., 1996) and summarized in Tables 1 and S1. These analyses were performed in duplicate.

2.2. Density fractionation

We applied a sequential density fractionation method to the soils following the procedure of Wagai et al. (2018). Sodium polytungstate (hereafter SPT solution, SPT-O grade, Sometu, Germany) was dissolved in deionized water to adjust the solution density to 1.6, 1.8, 2.0, 2.25, and 2.5 g cm^{-3}. Ten (10) grams of the soil sample was weighed in a 50 mL polypropylene tube and 35 mL of 1.6 g cm^{-3} SPT solution was transferred to the tube. After the mixture of soil and SPT solution was shaken for 1 h at 120 rpm on a reciprocal shaker, the tube was centrifuged with 3500 rpm for 20 min, and the material floating was collected on a 0.45 μm membrane filter (< 1.6 g cm^{-3} fraction). These steps were repeated three times to collect all materials in the target density fraction. The soil materials from < 1.6 g cm^{-3} fraction were rinsed with deionized water until the salt concentration reached < 50 mS cm^{-1}. Due to its insufficient recovery, this fraction (< 1.6 g cm^{-3}) was not included in this study. The residual soil materials after collecting < 1.6 g cm^{-3} fraction were mixed with 35 mL of 1.8 g cm^{-3} SPT solution, shaken and centrifuged using the same conditions as above. Floating materials (1.6–1.8 g cm^{-3} fraction, denoted as F1) were collected in the 250 mL centrifuge bottle and rinsed with deionized water until the salt concentration reached < 50 mS cm^{-1}. Using the same procedure to separate the 1.6–1.8 g cm^{-3} fraction, the remaining materials were fractionated to the density class of 1.8–2.0 (F2), 2.0–2.25 (F3), 2.25–2.5 (F4), and > 2.5 (F5) g cm^{-3} using the SPT solutions with 2.0, 2.25, and 2.5 g cm^{-3}. The collected materials from each density fraction were oven-dried at 40 °C and stored until further analysis.

The concentration of total P, Al, and Fe in each density fraction of both Andisols were obtained using the digestion method with H_2O_2-$HClO$-HNO_3-HF solution. The digestion was performed in duplicate. The concentration of Al, Fe, and Si extracted by pyrophosphate (Al_p, Fe_p, Si_p) and acid-ammonium oxalate (Al_{ox}, Fe_{ox}, Si_{ox}) in each density fraction of non-allophanic Andisols were sequentially obtained following the procedure of Asano and Wagai (2014). Elemental concentrations in the digests and extracts were analyzed using atomic absorption spectrometry (Z-5010, HITACHI High-Technologies, Japan) and ICP-AES

Table 1
Soil pH and elemental concentrations of Tsukuba (allophanic) and Kawatabi (non-allophanic) soils.

Soil	pH (H_2O)	Total C	Total N	Total P	Al_p	Al_d	Al_{ox}	Fe_p	Fe_d	Fe_{ox}
					g kg^{-1}					
Tsukuba	6.0	47.9	4.0	2.0	5.6	25.4	45.5	1.2	71.6	22.2
Kawatabi	6.0	90.4	5.8	2.0	16.6	16.7	19.6	6.2	19.5	9.8

pH: determind by a soil to solution ratio of 1:2.5.
Al_p and Fe_p: elements extracted by pyrophosphate solution extraction.
Al_d and Fe_d: elements extracted by dithionite solution extraction.
Al_{ox} and Fe_{ox}: elements extracted by oxalate solution extraction.

(SPECTRO ARCOS, HITACHI High-Technologies, Japan).

2.3. Chemical and sequential P fractionation

Phosphorus in the bulk soils and density fractions (except for < 1.6 g cm^{-3} fraction) were chemically extracted by referring to the methods by Hedley et al. (1982) and Hashimoto et al. (2014). A 0.2 g of each soil sample was weighed in a 50 mL polypropylene tube (n = 3). Phosphorus in the soil samples was extracted sequentially by 30 mL of deionized water (H_2O), 0.5 M $NaHCO_3$, 0.1 M NaOH, and 1.0 M HCl solutions for 16 h on a reciprocal shaker and supernatants were collected by centrifugation at 9000 rpm for 10 min. Supernatants were collected using a pipet, filtered by a 0.45 μm-membrane filter, and stored at 4 °C until chemical analyses. The concentration of molybdate-reactive P (P_i) in all soil extracts was determined colorimetrically by the ascorbic acid-phosphomolybdenum blue method using a UV spectrometer (Shimadzu Corporation, Japan). The concentration of total P (P_t) in each extract was determined by the same method used for P_i after the soil extracts were digested with a H_2SO_4-persulfate solution (Martin et al., 1999).

2.4. XANES spectroscopy

Phosphorus K-edge XANES measurements for the bulk soils and density fraction samples were conducted at Aichi Synchrotron Radiation Center (Aichi, Japan) using Beamline BL6N1 equipped with an InSb (1 1 1) monochromator at ambient temperature under a He atmosphere. References for P compounds and mineral adsorbed phases were also analyzed and summarized in SI. The XANES spectra for the samples and reference P compounds were collected in fluorescent yield mode. The P concentration was diluted to about 1% with boron nitride, if necessary. The monochromator was calibrated at the white-line (2481.7 eV) of K_2SO_4′s sulfur K-edge XANES spectrum. The background and baseline of all spectra were corrected and normalized using the Athena software (Ravel and Newville, 2005), and linear combination fitting (LCF) on the XANES spectra of samples was performed using all possible binary combinations of the P reference compounds with the best residual (R) value (see SI, Yamamoto and Hashimoto, 2017; Yamamoto et al., 2018). This fitting procedure can avoid a non-unique fitting solution because the use of a large number of standards inappropriately improve the R value (Hashimoto et al., 2014). Adding the third component to the LCF did not improve the R value. The P standard compounds used for LCF were P associated with Al [P adsorbed on gibbsite and allophane, and P associated with Al-OM data provided in Prietzel et al. (2016)], P associated with Fe (P adsorbed on ferrihydrite and goethite, and strengite), and P associated with Ca (hydroxyapatite and β-tri-calcium phosphate). The quality of LCF results was quantified through a residual R value, and the top three results of binary combinations of P standards were reported in SI. The LCF was performed in the relative energy range between −5 and 20 eV.

2.5. Solution ^{31}P NMR spectroscopy

Phosphorus species in the bulk soil and density fractionated soil samples (allophanic soil: F2, F3, and F4 groups, non-allophanic soil: F1, F2, and F3 groups) were analyzed using solution ^{31}P NMR in accordance with the method by Turner et al. (2003). One (1.00) gram of each sample was weighed in a 50 mL polypropylene tube (n = 2). Phosphorus in the soil samples was extracted by 20 mL of 0.25 M NaOH and 0.05 M EDTA mixture for 4 h on a reciprocal shaker and supernatants were collected by centrifugation at 9000 rpm for 30 min. Supernatants were collected using a pipet and filtered by a 0.45 μm-membrane filter. An aliquot of 3 mL was reserved for P_i and P_o determination. The remaining supernatants were pooled, frozen at −80 °C, and lyophilized for the NMR analysis. The lyophilized sample was ground with a mortar and pestle, and 100 mg was weighed in a 5 mL tube. The sample was dissolved in 0.9 mL of 1.0 M NaOH and 0.1 mL of D_2O, and the solution was transferred to a NMR tube. The sample dissolution was done within 30 min before starting the NMR data acquisition. Solution ^{31}P NMR spectra were obtained using JEOL ECA-500 spectrometer (JEOL Ltd., Japan). The NMR parameters were a 45° pulse (6 μs), a delay time of 1 s, an acquisition time of 2.58 s, and 6800–22000 scans at 22 ± 1 °C. The NMR data were processed using the JEOL software, Delta 5.0.4 (JEOL Ltd., Japan). All NMR spectra were processed with a line broadening of 2 Hz and the inorganic *ortho*-P signal was adjusted to 6.0 ppm. Signals of NMR spectra were grouped into P species including orthophosphate, mono- and diesters, and pyrophosphate following previous studies (Turner et al., 2003).

3. Results

3.1. Characterization of bulk soils

The basic soil properties of Tsukuba (allophanic Andisols) and Kawatabi (non-allophanic Andisols) soils are shown in Table 1. The pH (H_2O) value and total P in the Tsukuba soil were similar to Kawatabi soil. The total C in the Tsukuba soil was about half of the Kawatabi soil, and the total N in the former was also lower than that in the latter. The concentration of oxalate extractable Al (Al_{ox}) and Fe (Fe_{ox}) in the Tsukuba soil was > 2 folds higher than the Kawatabi soil, whereas pyrophosphate extractable Al (Al_p) and Fe (Fe_p) in the former was less than half of the latter. The extraction efficiency of organo-Al/Fe complexes by pyrophosphate and short-range-order Al and Fe minerals by acid-ammonium oxalate was estimated to be between 80% and 100% (Wagai et al., 2013). The Tsukuba soil was enriched with short-range-order Al and Fe minerals (i.e., oxalate extractable phase) (Borggaard, 1992; Parfitt and Childs, 1988), but was scarce in organo-Al/Fe-complexes (i.e., pyrophosphate extractable phase) (Loveland and Digby, 1984; Parfitt and Childs, 1988) relative to the Kawatabi soil (Hashimoto et al., 2012; Shoji and Fujiwara, 1984; Wagai et al., 2013).

3.2. Characterization of density fractions

Fig. 1 shows the mass distribution (% w/w) of each density fraction to the total soil mass. The soil mass recovery (i.e., the sum of the isolated fractions including < 1.6 g cm^{-3} fraction) was 107% for the Tsukuba soil and 95% for the Kawatabi soil. In the Tsukuba soil, the 2.0–2.25 g cm^{-3} fraction (F3) contained the largest proportion of mass (44%), followed

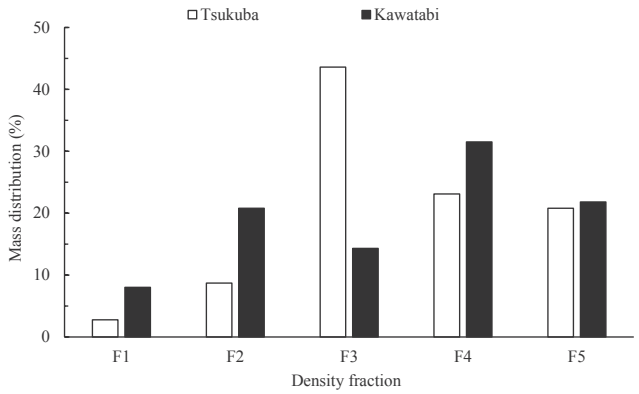

Fig. 1. Mass distribution (% w/w) of density fractions of Tsukuba (allophanic) and Kawatabi (non-allophanic) soils. F1: 1.6–1.8 g cm^{-3}, F2: 1.8–2.0 g cm^{-3}, F3: 2.0–2.25 g cm^{-3}, F4: 2.25–2.5 g cm^{-3}, F5: > 2.5 g cm^{-3}.

by the 2.25–2.5 g cm^{-3} fraction (F4, 23%) and the > 2.5 g cm^{-3} fraction (F5, 21%). These fractions accounted for 88% of the total soil mass. In the Kawatabi soil, the F4 (32%) accounted for the largest proportion, followed by F5 (22%) and F2 (1.8–2.0 g cm^{-3}, 21%).

Fig. 2 shows the concentrations of total and extracted elements in the density fractions of Tsukuba and Kawatabi soils. The P concentration in density fractions of Tsukuba soil was mainly distributed from F2 to F3 (1.8–2.25 g cm^{-3}) fractions, accounting for 55% of the sum of P from F1 to F5 (Fig. 2b). In the Kawatabi soil, F1 and F2 (< 2.0 g cm^{-3}) were the primary sinks of P, accounting for 64% across the entire density ranege (Fig. 2b). Accumulation of P was less pronounced in the higher-density fractions (F4 and F5) of Kawatabi soil than those of Tsukuba soil (Fig. 2b). Overall, the distribution of P along the density fraction was different between the Tsukuba and Kawatabi soils where P accumulation occurred preferentially in the lower-density fractions for Kawatabi (non-allophanic) than Tsukuba (allophanic). By the multiplication of total P in each density fraction by the weight of each density fraction, the recovery of P with the density fractionation was found to be 91% for Tsukuba and 93% for Kawatabi. Therefore, the high P recovery indicated that the SPT solution used for the density fractionation of soils did not significantly affect P loss.

The pyrophosphate-extractable Fe and Al (Fe_p and Al_p) concentrations in the Kawatabi soil also showed density-dependent trends with a greater concentration in the lower-density fractions (F1 and F2, < 2.0 g cm^{-3}) than the higher-density fractions (Fig. 2c, e). In contrast, these metal concentrations in the Tsukuba soil was relatively constant at around 5 g kg^{-1} and 3 g kg^{-1} along the density gradient, respectively. The concentrations of Feox in F1 and F2 were similar between the Tsukuba and Kawatabi soils (14–22 g kg^{-1}), whereas Fe_{ox} in the higher-density fractions in the Kawatabi soil (F4 and F5, > 2.25 g cm^{-3}) was notably less than those of Tsukuba soil (Fig. 2d). The concentration of Al_{ox} increased with density and reached a maximum level of 67 g kg^{-1} at F3 (2.0–2.25 g cm^{-3}) in the Tsukuba soil; contrastingly, Al_{ox} in the Kawatabi soil decreased from 42 g kg^{-1} to 7.0 g kg^{-1} with increasing density from F1 to F5 (Fig. 2f). The difference in the relative dominance of pyrophosphate and oxalate extractable metal phases between the Tsukuba (allophanic) and Kawatabi (non-allophanic) soils were clearly shown by comparing the ratio of Al_p to Al_{ox} and Fe_p to Fe_{ox} along the density gradient (Fig. S1). The ratios of Fe_p/Fe_{ox} and Al_p/Al_{ox} in the Tsukuba soil were constant around 0.3 and 0.07, respectively, whereas those ratios in the Kawatabi soil were remarkably higher around 0.8 in the lower-density fractions (1.6–2.25 g cm^{-3}). Regardless of density, Si_{ox} concentrations were consistently higher in the Tsukuba soil (4.4–29 g kg^{-1}) than the Kawatabi soil (0.8–2.1 g kg^{-1}) (Fig. 2h), indicating the abundance of allophane/imogolite type minerals in the former than the latter (Wagai et al., 2020).

3.3. Sequentially extracted P

Fig. 3 shows the concentration of molybdate-reactive P (P_i) and the sum of molybdate-reactive and unreactive P (P_t) in sequential extracts of bulk soils and density fraction samples. A large portion of P_t was determined in the NaOH extracts of the bulk soil of Tsukuba and Kawatabi (Fig. 3). Molybdate-reactive P in the bulk soil of Tsukuba and Kawatabi was mostly extracted by the NaOH fluid, accounting for 89% (1.1 g kg^{-1}) and 75% (0.9 g kg^{-1}) of the sum of P_i in sequential extracts, respectively. Phosphorus extracted by the NaOH fluid is considered as P associated with Al and Fe bearing minerals and (oxyhydr)oxides (Hedley et al., 1982), indicating that P in the Tsukuba and Kawatabi soils consisted mainly of Fe and Al-bound forms. The residual P was the second largest fraction in the bulk soils of Tsukuba (12%, 0.3 g kg^{-1}) and Kawatabi (17%, 0.4 g kg^{-1}) (Fig. 3). Phosphorus extracted by the HCl fluid, which is considered as apatite-like minerals, was minor in the Tsukuba and Kawatabi soils accounting for < 6% (< 0.2 g P_i kg^{-1}) of total P. A difference in P_t between the Tsukuba and Kawatabi soils was found in the $NaHCO_3$ extract in which P in the latter (15%, 0.3 g kg^{-1}) was greater than the former (5%, 0.1 g kg^{-1}). Phosphorus extracted by the $NaHCO_3$ fluid is considered readily soluble P (Hedley et al., 1982), suggesting that Kawatabi may contain more bioavailable P compared to Tsukuba.

Similar to the bulk soils, P_i extracted by NaOH was the primary pool in all density fractions of the Tsukuba and Kawatabi soils. The NaOH-P_t was also the primary pool from F1 to F4 of Tsukuba soil and from F1 to F3 of Kawatabi soil (Fig. 3). However, the proportion of residual P to the total P was prominent in F5 of Tsukuba (0.4 g kg^{-1}, 52%) and F4 and F5 of Kawatabi (0.6 g kg^{-1}, 66–83%). With increasing density from 1.6 to 2.5 g cm^{-3}, the percentage of the residual P to the total P increased from 0% to 52% in Tsukuba and from 12% to 83% in Kawatabi. The result indicated that the NaOH-P pool in the Tsukuba and Kawatabi soils was derived from the lower-density fractions (< 2.25 g cm^{-3}), whereas their residual P pools were derived from the higher-density fractions (> 2.25 g cm^{-3}). The HCl-P pool in the bulk soils of Tsukuba and Kawatabi was distributed across the entire density range. The $NaHCO_3$-P pool in the Kawatabi soil was mainly distributed from F1 to F3, but that in the Tsukuba soil was almost uniformly distributed across the density fractions.

3.4. Phosphorus K-edge XANES spectroscopy

Fig. 4 shows the P K-edge XANES spectra of bulk soils and selected density fractions for Tsukuba and Kawatabi together with the results of LCF with P standard spectra. All XANES spectra of bulk samples and density fractions for Tsukuba and Kawatabi were characterized by a distinct white-line peak at 2150 eV and were similar to the standard spectra of P associated with Al (e.g., P associated with allophane and gibbsite). There was no pre-edge feature around 2145 eV in all XANES spectra, indicating that P associated with Fe was minor in the bulk soils and density fractions (Hesterberg et al., 1999). In the bulk soil of Kawatabi, a feature indicating hydroxyapatite or P associated with Ca was found at the shoulder on the high-energy side of the white-line peak (Hashimoto et al., 2014; Yamamoto et al., 2018). The visual observation on the XANES spectra suggested therefore that P associated with Al were the primary P species in the bulk and density fractions of Tsukuba and Kawatabi. Because of high similarity in P K-edge XANES spectra between minerals and adsorbed phases (e.g., variscite vs. P adsorbed on gibbsite and allophane), the LCF results were grouped and reported as P associated with Al (Al-P), Ca (Ca-P) and Fe (Fe-P) (Yamamoto and Hashimoto, 2017). Moreover, we used XANES data to determine inorganic phosphate species in the samples because P K-edge XANES is not always appropriate for organic P identification in soils (Hesterberg, 2010; Yamamoto et al., 2018).

The results of LCF demonstrated that the Tsukuba soil (bulk) contained 100% P associated with Al. The second- and third-best results of

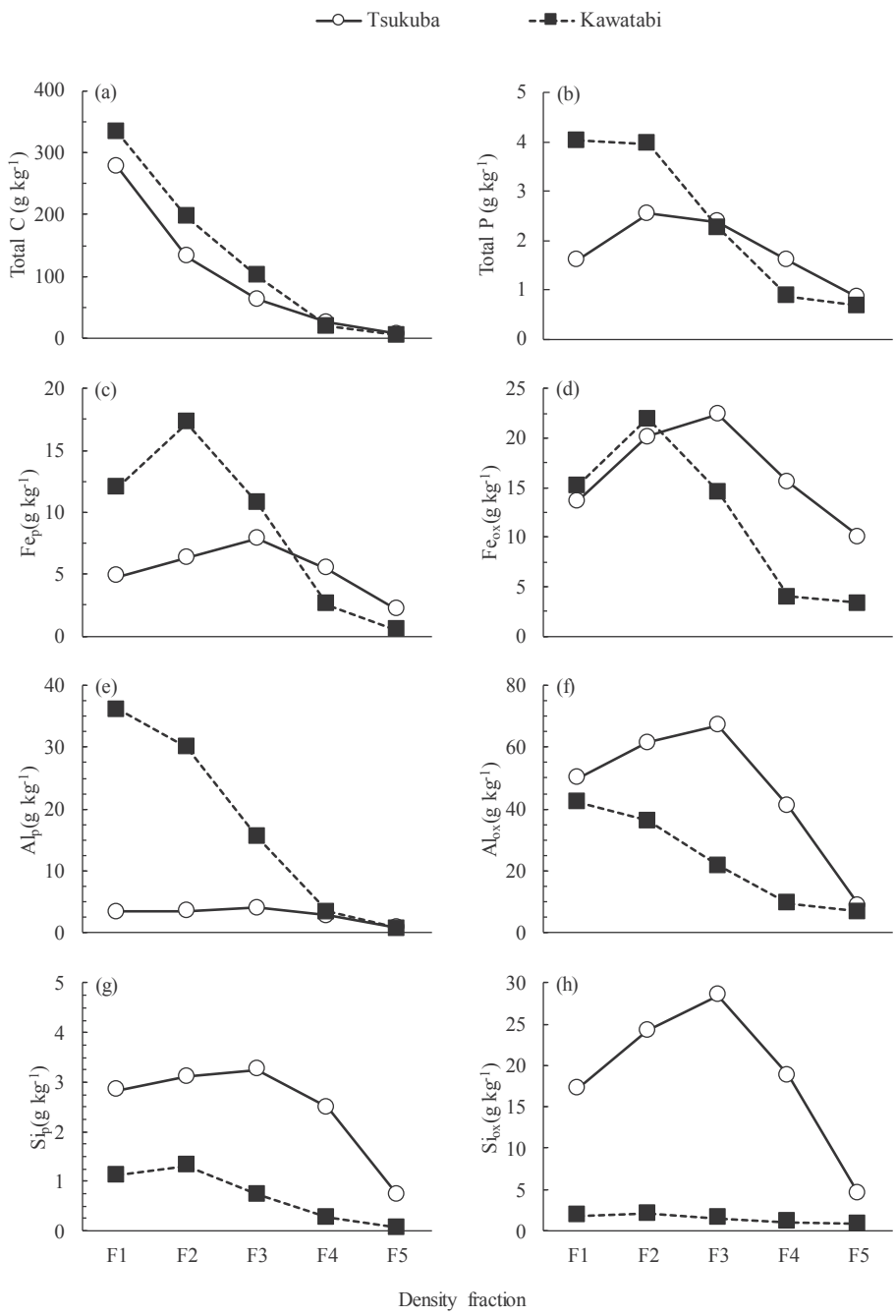

Fig. 2. Concentrations of total C, total P, Fe_p, Fe_{ox}, Al_p, Al_{ox}, Si_p, and Si_{ox} from low- to high-density fractions of Tsukuba (allophanic) and Kawatabi (non-allophanic) soils. For the Tsukuba soil, the data were reported in Wagai et al. (2020). F1: 1.6–1.8 g cm^{-3}, F2: 1.8–2.0 g cm^{-3}, F3: 2.0–2.25 g cm^{-3}, F4: 2.25–2.5 g cm^{-3}, F5: > 2.5 g cm^{-3}.

LCF on the Tsukuba soil (Table S4) showed a minor contribution of Fe-P species (e.g., P associated with ferrihydrite, < 20%), suggesting that the presence of Fe-P cannot be completely ruled out, but P was mainly associated with Al in the Tsukuba soil. The Tsukuba density fractions with high P concentrations (F2, F3, and F4) were also analyzed for P K-edge XANES, which showed that P associated with Al was the primary species in the best-, second-best and third-best results of LCF (Table S4). In the bulk soil of Kawatabi, P associated with Al was the primary species (77%) and a lesser extent of P associated with Ca (23%). According to the second- and third-best results of LCF, P associated with Ca was determined as a secondary P species in the bulk soil of Kawatabi (Table S5). Calcium-bound P was probably derived from Ca phosphate fertilizer repeatedly applied in the field. The Kawatabi density fractions with high P concentrations (F1, F2, and F3) were also analyzed for P K-edge XANES and found that P associated with Al was the primary species in the best-, second-best and third-best results of LCF (Table S5). Phosphate associated with Ca was very minor in F1, F2, and F3 samples of Kawatabi soil, although it occurred in the bulk soil. Phosphate associated with Ca may be distributed in heavier fractions of Kawatabi soil since Ca-phosphate minerals (e.g., hydroxyapatite) generally have a high particle density with > 3 g cm^{-3}. Overall, P in the Tsukuba (allophanic) and Kawatabi (non-allophanic) soils and their density fractions was mainly associated with Al that was likely derived from gibbsite, allophane, and organo-Al complexes (discussed later).

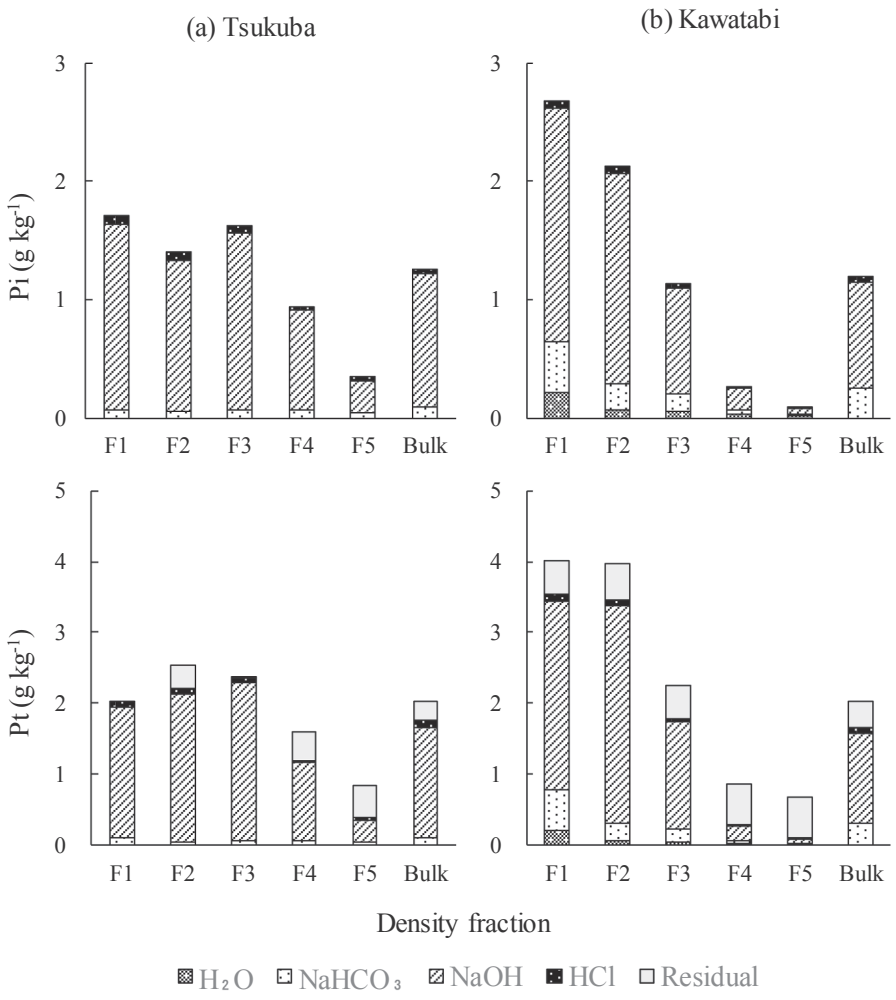

Fig. 3. Molybdate-reactive P (P_i) and total P (P_t) in H2O, NaHCO3, NaOH, HCl and residual pools of bulk soils and density fractions of (a) Tsukuba (allophanic) and (b) Kawatabi (non-allophanic). F1: 1.6–1.8 g cm^{-3}, F2: 1.8–2.0 g cm^{-3}, F3: 2.0–2.25 g cm^{-3}, F4: 2.25–2.5 g cm^{-3}, F5: > 2.5 g cm^{-3}.

3.5. Solution ^{31}P NMR spectroscopy

The results of solution ^{31}P NMR were mainly focused on organic P species in the bulk soils and selected density fractions with high P concentrations (Fig. 5 and Table 2). The P recovery of NaOH-EDTA soil extracts from the bulk soils and density fraction samples used for the NMR measurement ranged from 27% to 71% for Tsukuba and from 45% to 87% for Kawatabi. The P recovery of NaOH-EDTA extracts were lower in the density fractions (40 ± 18%) than in the bulk soils (79 ± 11%). The low P recovery from NaOH-EDTA extracts of density fraction samples suggests that the results from NMR should be carefully interpreted with an emphasis on qualitative viewpoints for organic P species.

The proportions of inorganic orthophosphates (*ortho*-P) in Tsukuba soil (bulk, 83%) was higher than that in the Kawatabi soil (bulk, 72%) (Table 2). In the Tsukuba density fractions, the proportions of *ortho*-P increased from 69% to 88% with increasing density from F2 to F4 (1.8–2.5 g cm^{-3}) (Table 2). A similar trend in *ortho*-P from F1 to F3 (1.6–2.25 g cm^{-3}) was observed in the density fractions of Kawatabi (Table 2). The primary organic P group in the bulk soils was phosphomonoesters (P-monoesters), accounting for 13% in Tsukuba, and 28% in Kawatabi (Table 2). The proportions of P-monoesters in the density fractions decreased with increasing density in which P-monoesters decreased from 28% (F2) to 10% (F4) in Tsukuba and from 42% (F1) to 35% (F3) in Kawatabi. This decreasing trend corresponded to the concentration of organic P extracted by NaOH-EDTA (Table S6). In the Kawatabi bulk soil, F2 (1.8–2.0 g cm^{-3}) and F3 (2.0–2.25 g cm^{-3}), the signals indicative of *myo*-inositol hexakisphosphate (*myo*-IHP) were identified around 4.43, 4.55, 4.92, and 5.85 ppm in the P-monoester region of NMR spectra (Fig. 5). The signals associated with *scyllo*-IHP (4.02–4.2 ppm) were also identified in bulk, F1, F2, and F3 (1.6–2.25 g cm^{-3}) samples of Kawatabi soil (Fig. 5). Previous studies reported *scyllo*-IHP in a tundra area soil at Dovrefjell (Turner and Richardson, 2004), but it was less frequently found in soils relative to *myo*-IHP. Contrarily, the signals associated with *myo*-IHP and *scyllo*-IHP were not clearly exhibited in the bulk soil and density fractions of Tsukuba relative to those in Kawatabi. A signal associated with pyrophosphates (-4.3 ppm) were not identified in the bulk soil and density fractions of Kawatabi, whereas it was observed in the bulk soil and density fractions of Tsukuba around < 4% of the total P. Signals associated with polyphosphates (-3.9 ppm) and phosphodiesters (-3.0–2.5) were absent for the Tsukuba and Kawatabi samples.

4. Discussion

4.1. Distribution of P in relation to Al and Fe in density fractions

Allophanic and non-allophanic Andisol samples used in this study were characterized by contrasting mineralogy in oxalate and pyrophosphate extractable Al and Fe. The allophanic Andisols (Tsukuba) with high in Al_{ox} and Fe_{ox} suggest that Al and Fe in the density fractions of Tsukuba soil were likely to be present as short-range-ordered or poorly-crystalline phases (Parfitt and Childs, 1988; Rennert, 2019). In

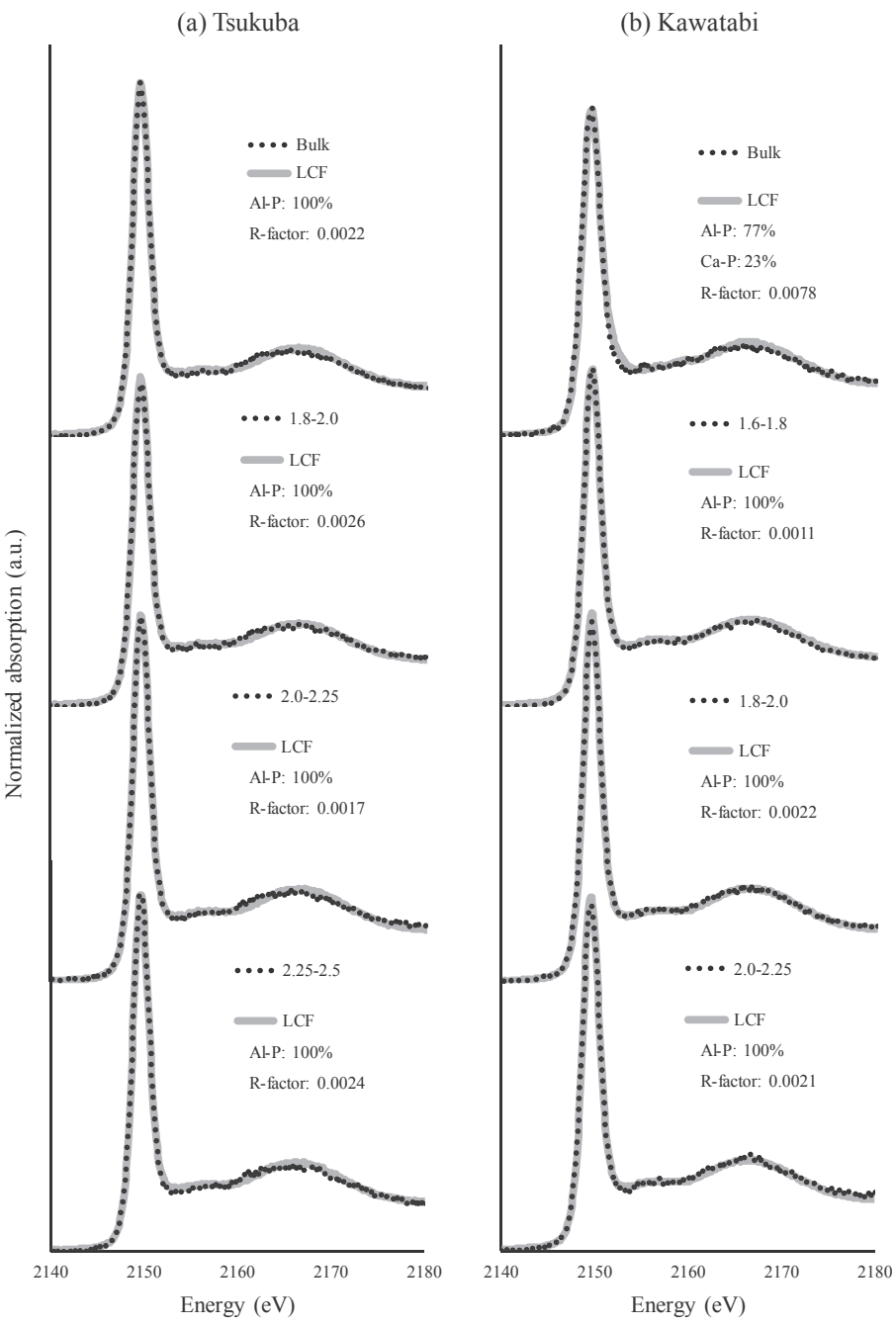

Fig. 4. Phosphorus P K-edge XANES spectra of bulk soils and selected density fractions (dotted black lines), and their linear combination fitting (LCF) using the reference spectra (solid gray lines). (a) Tsukuba (allophanic) soils: bulk, 1.8–2.0 g cm^{-3} (F2), 2.0–2.25 g cm^{-3} (F3), 2.25–2.5 g cm^{-3} (F4). (b) Kawatabi (non-allophanic) soils: bulk, 1.6–1.8 g cm^{-3} (F1), 1.8–2.0 g cm^{-3} (F2), 2.0–2.25 g cm^{-3} (F3). Al-P: P associated with Al. Ca-P: P associated with Ca (see SI for the LCF results in detail).

contrast, the non-allophanic Andisols (Kawatabi), especially in the lower-density fractions, were enriched with Al_p and Fe_p, suggesting the abundance of organo-Al/Fe complexes (Bascomb, 1968; Takahashi and Dahlgren, 2016) with some inevitable inclusion of colloidal Al and Fe phases (Coward et al., 2018; Kaiser et al., 1996; Schuppli et al., 1983).

The distribution of P across the density fractions was contrasting between allophanic (Tsukuba) and non-allophanic (Kawatabi) Andisols. We found that soil P in Tsukuba was most abundant in the *meso*-density fraction (F2 and F3, 1.8–2.25 g cm^{-3}) (Fig. 2b). The distribution pattern of P concentration along the density gradient (Fig. 2b) corresponded to that of Al_{ox} concentrations in the Tsukuba soil (Fig. 2f). The concentration of Al_{ox} in the Tsukuba soil positively correlated with P_i and P_t extracted by NaOH across the density fractions (r = 0.91–0.98; Table S3). Besides, the distribution of Si_{ox} closely followed that of Al_{ox} with an Al/Si ratio of 2–3. These results strongly suggest that short-range-order aluminosilicates (e.g., allophane) contributed to P distribution in density fractions of Tsukuba soil. In contrast, the lower-density fractions (F1 and F2, 1.6–2.0 g cm^{-3}) were the major pools of P_i and P_t in the Kawatabi soil (Fig. 2b). The Al_p, instead of Al_{ox}, across the density fractions of Kawatabi soil (Fig. 2e) correlated strongly with NaOH extracted P_i and P_t ($r > 0.97$, Table S3), indicating the strong contribution of Al_p phase to P distribution in each density fraction. The density of organo-Al coprecipitates experimentally synthesized is <2.0 g cm^{-3}, and that of Al hydroxide is >2.0 g cm^{-3}, even with sorbed OM at maximum levels (Kaiser and Guggenberger, 2007). Furthermore, NaOH-P_i and -P_t in density fractions of Tsukuba and Kawatabi soils positively correlated with Fe_{ox} (r = 0.68–0.90) and Fe_p (r = 0.79–0.97), but the NaOH-P_i and -P_t correlated more strongly with Al_{ox} ($r > 0.98$) and Al_p ($r > 0.94$) (Table S3). These findings, therefore, suggest that a large proportion of P stored in < 2.0 g cm^{-3} fractions of Kawatabi is likely to be bound to monomeric or polynuclear Al phases, some of which may be complexed with organic ligands. It should be noted however that

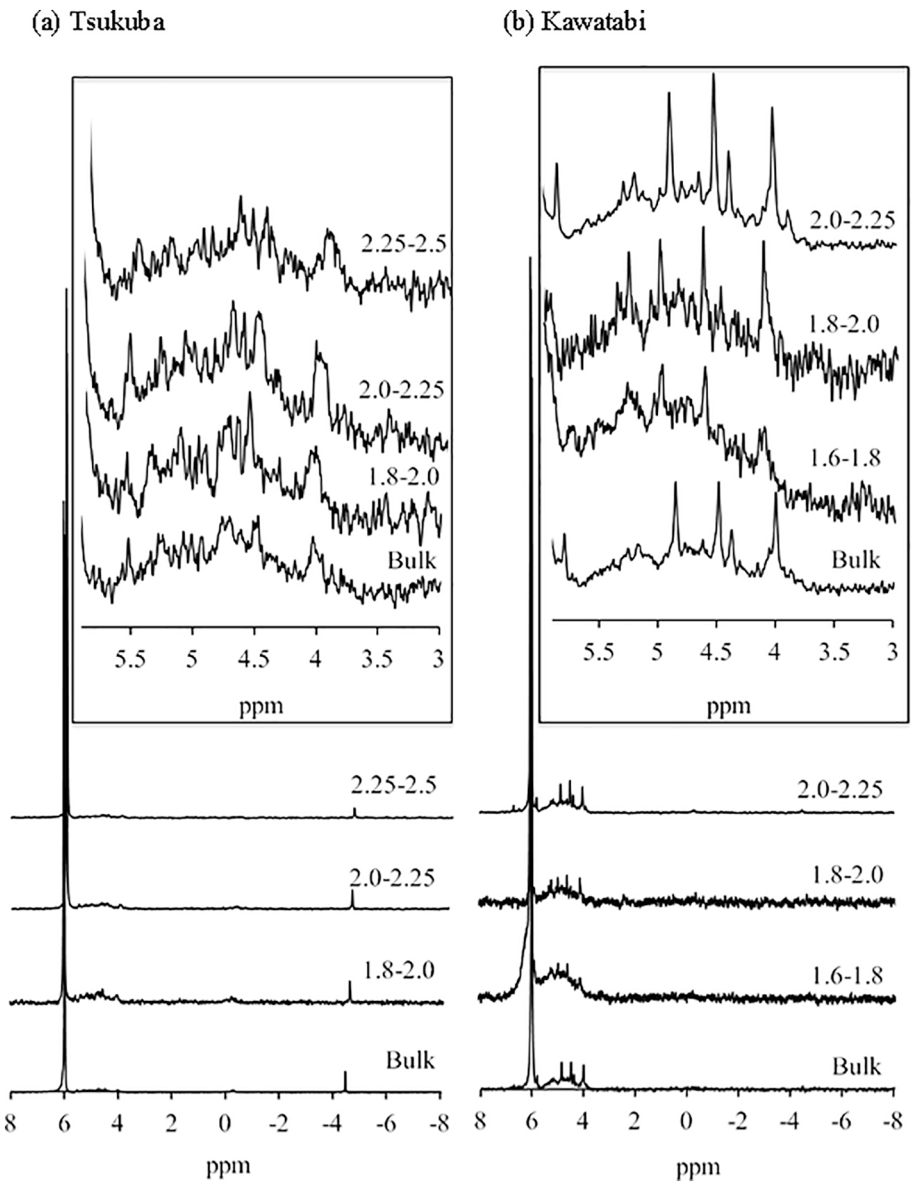

Fig. 5. Solution ^{31}P NMR spectra of NaOH-EDTA extracts of bulk soils and selected density fractions for (a) Tsukuba (allophanic) and (b) Kawatabi (non-allophanic) soils. (a) bulk, 1.8–2.0 g cm^{-3} (F2), 2.0–2.25 g cm^{-3} (F3), 2.25–2.5 g cm^{-3} (F4). (b) bulk, 1.6–1.8 g cm^{-3} (F1), 1.8–2.0 g cm^{-3} (F2), 2.0–2.25 g cm^{-3} (F3). A magnified scale in the phosphomonoester region is shown in the boxes.

Table 2
Concentrations and relative percentage (in parentheses) of P_i and P_o groups in NaOH-EDTA extracts of bulk and density fractions for Tsukuba (allophanic) and Kawatabi (non-allophanic) soils determined by solution ^{31}P NMR spectroscopy.

Density fraction	P_i Orthophosphate	Pyrophosphate	Polyphosphate	P_o Monoester	Diester
			g kg^{-1} (%)		
			Tsukuba		
F2	0.5 (69.0)	0.02 (3.1)	0	0.2 (28.0)	0
F3	0.8 (80.4)	0.03 (2.8)	0	0.2 (16.8)	0
F4	0.5 (87.6)	0.01 (2.0)	0	0.1 (10.4)	0
Bulk	1.2 (83.1)	0.05 (3.8)	0	0.2 (13.1)	0
			Kawatabi		
F1	1.0 (57.2)	0	0	0.8 (42.8)	0
F2	1.5 (66.8)	0	0	0.7 (33.2)	0
F3	1.1 (64.6)	0	0	0.6 (35.4)	0
Bulk	1.3 (71.7)	0	0	0.5 (28.3)	0

Chemical shifts correspond to orthophosphate (6 ppm)pyrophosphate (-4.3 ppm), polyphosphate (-3.9 ppm), orthophosphate monoesters (6.4–7.7, 2.9–5.7 ppm), and orthophosphate diesters (-3–2.5 ppm).

evidence based on spectroscopy is necessary to conclude that either Al or Fe plays a primary role in P sorption and distribution in the density fractions of allophanic and non-allophanic Andisols (described later).

Our results highlight the quantitative importance of residual P pool across density fractions of Andisols. This agrees with the fact that the residual pool remaining after the sequential extraction still contained a significant amount of P with up to 63% of total soil P (Velásquez et al., 2016), some of which were available to plant uptake (Condron and Newman, 2011; Schubert et al., 2020). The combination uses of sequential extraction and density fractionation revealed that the percentage of residual P to total P progressively increased with increasing density in which F4 and F5 fractions (> 2.25 g cm^{-3}) of both Andisols were the primary sink for the residual P (Fig. 3). The residual P reached a maximum level at F5 fraction (Tsukuba 52%, Kawatabi 83%). Compared to the rest of density fractions, F5 contained lower concentrations of oxalate and pyrophosphate extractable Al, Fe and Si (Fig. 2), and these parameters negatively correlated with residual P concentrations across density fractions of both Andisols (Table S3). In addition, the lower concentration of Al_{ox} and Fe_{ox} in F4 and F5, relative to the lighter density fractions, suggests that soil P in the residual pool is not only associated with Al/Fe bearing minerals and oxides but also forms organo-Al/Fe complexes. The residual pool after HCl extraction contained occluded P with crystallized Al or Fe minerals (Gu et al., 2020; Smeck, 1985; Takamoto and Hashimoto, 2014), also suggesting the importance of crystalline Al and Fe minerals and oxides for stabilization of P in soils. It has been reported that residual P is distinctive of highly weathered soils or old soils (Turner and Laliberté, 2015; Velásquez et al., 2016). Our results shed light on this mechanism that highly weathered soils are characterized by a large proportion of heavy density fractions (Sollins et al., 2009; Wagai et al., 2008), and therefore heavy density fractions serve as important sinks of soil residual P together with crystalline Al and Fe minerals.

4.2. Molecular-level characteristics of inorganic P

The XANES spectroscopy revealed that P in the bulk soils and the density fractions of Tsukuba and Kawatabi soils was primarily associated with Al rather than Fe or Ca (Fig. 4). A large number of studies on P in Andisols reported a significant positive correlation between extractable P and oxalate and pyrophosphate extractable Al and Fe (Gunjigake and Wada, 1981; Hashimoto et al., 2012; Matsuyama, 1994; Nanzyo et al., 1993; Percival et al., 2000). Previous studies using wet chemical analyses have deduced that Al and Fe (oxy)hydroxides, allophane and organo-Al/Fe complexes play important roles in P sorption in various types of Andisols (Gunjigake and Wada, 1981; Hashimoto et al., 2012; Matsuyama, 1994; Nanzyo et al., 1993; Percival et al., 2000). However, it has long been unknown whether either Al or Fe has a primary role in P sorption and fractionation in Andisols. Our study using XANES spectroscopy unambiguously determined that Al is more crucial than Fe for P sorption in allophanic and non-allophanic Andisols at bulk and density-fraction levels. While further studies with a larger number of samples are necessary, the nature of P accumulation revealed by the current study may be applicable to other Andisols for two reasons. First, the two soils studied here are considered as typical of Japanese allophanic and non-allophanic Andisols (Asano and Wagai, 2014; Saigusa et al., 1994; Shoji and Fujiwara, 1984; Wagai et al., 2013). Second, our finding based on XANES spectroscopy is in good agreement with the results from the multivariate analysis on extraction data across 650 Andisol samples, demonstrating that Al_{ox} and Al_p are more critical than Fe_{ox} to characterize soil P accumulation (Hashimoto et al., 2012).

There has been a long debate on the significance of organo-Al complex on P accumulation in Andisols high in OM. The concentration of organo-Al complexes, assumed to be soluble in a sodium-pyrophosphate reagent (Nanzyo et al., 1993; Percival et al., 2000; Takahashi and Dahlgren, 2016), strongly correlated with P sorption capacity particularly in non-allophanic Andisols (Gunjigake and Wada, 1981; Hashimoto et al., 2012). Increased P sorption in organic-rich soils is often attributed to the formation of organo-Al complexes that may provide positively-charged reactive sites for P sorption (Giesler et al., 2005). A presumed mechanism of P binding in OM-rich soil or fraction is the formation of ternary complexes with Al (or Fe) where a bridging metal is centered between P and organic functional groups (Gerke, 2010; Hesterberg, 2010). Previous studies using P K-edge XANES spectroscopy identified P associated with organo-Al in Cambisol samples (Giguet-Covex et al., 2013; Werner et al., 2017). Our results demonstrated that the XANES standard spectra of P associated with organo-Al complexes differed in fine structure from those of P associated with gibbsite and allophane (Fig. S2). Such differences in P-XANES spectra yielded P associated with organo-Al as a primary or secondary component of P species in Tsukuba and Kawatabi soils (Tables S4, S5). A striking feature of Kawatabi soil was that P associated with organo-Al complex was consistently identified as the primary component ($> 62\%$ of total P) in the best-, and second-best results of LCF in density fraction samples (Table S5). The proportion of P associated with organo-Al complex reached 76% in the lowest-density fraction of Kawatabi (F1, 1.6–1.8 g cm^{-3}) in which the highest P concentration was found across density fractions (Table S5). These findings highlight the probable presence of P associated with organo-Al complexes that have been conceptually presumed and considered to be critical components in the high P accumulation of Andisols. Further studies are needed, however, to clarify the entire picture of P associated with organo-Al complexes with complementary use of spectroscopic and wet chemical analyses.

4.3. Organic phosphates in bulk soils and density fractions

Phosphomonoester was most predominant in the low-density fraction of Tsukuba (F2, 28%) and Kawatabi (F1, 43%) and was illustrated by the broad signals of their ^{31}P NMR spectra between 7.0 and 3.5 ppm (Fig. 5 and Table 2). The occurrence of the broad resonance in the phosphomonoester region of NMR is associated with i) the presence of multiple organic P species (Doolette et al., 2011), ii) concentrated paramagnetic metal ions in soil extracts (Cade-Menun and Liu, 2014), and iii) the presence of P bound to phosphomonoester linking with polymeric materials (McLaren et al., 2015). The P species consisting of the broad resonance in the phosphomonoester region are conceptualized as humic-P (Doolette et al., 2011) or organic P compounds with supra-/macro-molecular structures (McLaren et al., 2015), although their molecular structures remain unknown. McLaren et al. (2015) pointed out that phosphomonoesters with supra-/macro-molecular structures were the major soil organic P in various soils, and therefore suggested their significance for the elucidation of P cycles in terrestrial ecosystems. We found the preferential accumulation of these soil phosphomonoesters in the lower-density fractions where soil OM is less microbially altered and the mean residence time of C is much shorter compared to higher-density fractions (Sollins et al., 2009, 2006; Wagai et al., 2018). These results suggest the potential significance of relatively fresh, plant-derived OM in organic P accumulation and the importance of interpreting soil P dynamics in relation to C and N.

Myo-IHP and *scyllo*-IHP, which are categorized in the phosphomonoester group, were identified in the bulk soil and density fractions of Kawatabi soil. The result of ^{31}P NMR illustrated a remarkable accumulation of *myo*-IHP and *scyllo*-IHP in the *meso*-density fraction (F3, 2.0–2.25 g cm^{-3}) relative to the lower-density fractions of Kawatabi. It has been known that IHP or phytic acid is strongly adsorbed to the surfaces of iron oxides (De Groot and Golterman, 1993), and non-crystalline Al or Fe precipitates (Shang et al., 1992). Borie et al. (1989) reported that significant amounts of IHP are associated with humic and fulvic acid fractions. IHP has been recognized as a stable organic P form with low biodegradability (Giaveno et al., 2010; Martin et al., 2004). Giaveno et al. (2010) reported that IHP associated with Fe and Al minerals retarded biological degradation due to the limited activity of phosphomonoesterases. More recently, Wagai et al. (2020)

showed that *meso*-density fractions (1.8–2.4 g cm^{-3}) were characterized by microaggregates that were held together by OM and reactive Fe and Al phases across soils including non-allophanic Andisols. Our results, therefore, suggest the preferential accumulation of IHP in the *meso*-density fraction of Kawatabi soil may be attributable to the protective role of extractable Al and Fe phases in chemical or physical means.

5. Concluding remarks

We investigated the density distribution and molecular characterization of P in the bulk soil and density fractions for one allophanic and one non-allophanic Andisols. Dominant portions of P were found in the *meso*-density fraction (F2 and F3, 1.8–2.25 g cm^{-3}) for the allophanic Andisol and low-density fractions (F1 and F2, 1.6–2.0 g cm^{-3}) for the non-allophanic Andisol. The trend of P distribution along the density gradient corresponded to Al_{ox} and Fe_{ox} for the allophanic Andisol (Tsukuba) and to Al_p for the non-allophanic Andisol (Kawatabi). The XANES spectroscopy further revealed that P in both Andisols was associated mainly with Al phases (e.g., gibbsite and allophane) but the non-allophanic Andisols appeared to show phosphate-Al-OM linkages. Phosphomonoesters were the major group of organic P in both Andisols and increased their abundance with decreasing particle density. We also found a clear localization of *myo*-IHP and *scyllo*-IHP in the *meso*-density fraction of Kawatabi soil. Overall, low to *meso*-density fractions between 1.6 and 2.25 g cm^{-3} were the main P reservoirs in the allophanic and non-allophanic Andisoils used in this study. Using 23 soil samples from various pedons, Wagai et al. (2020) revealed that *meso*-density fractions were the primary sink of oxalate and pyrophosphate extractable Al and Fe. Besides Andisols, it is therefore suggested that the *meso*-density fractions of soils play a central role in accumulation of P in the other pedons, and the mechanisms involved in P dynamics and fractionation in soils may be revealed with a strong focus on the *meso*-density range.

The novel combination of density fractionation, chemical extraction, and spectroscopy-based molecular-level characterization of P used here revealed new mechanistic insights on P forms in Andisols and possibly in other soils. The results suggest new evidence of the ternary association of P (i.e., phosphate-Al-OM linkages) in Andisols based on the combination of selective metal extraction and XANES spectroscopy. The preferential stabilization of *myo*-IHP and *scyllo*-IHP in the *meso*-density fraction has not been reported previously. Whether these reactions are unique to non-allophanic Andisols or present in other systems rich in OM and reactive Al phases (e.g., spodic horizons, rhizosphere, sediments in water treatment plants) needs to be substantiated. We also found more significant roles of Al phases on soil P sorption and fractionation relative to Fe phases, whereas it remains unclear which soil chemical and pedogenic factors control the relative importance of Al over Fe on P sorption in allophanic and non-allophanic Andisols. Our Andisols also showed major storage of C (Fig. 2a) and N (data not shown) in the low- to *meso*-density fractions that occurred in concert with high P accumulation (Fig. 2b), highlighting the prominent role of the lower-density fractions in the cycling of C, N and P. The current approach revealed new insights on metal (esp. Al) controls on P and C-N-P interactions and therefore would be a promising approach for better understanding of biogeochemical cycling of P.

Declaration of Competing Interest

The authors declare that they have no known competing financial interests or personal relationships that could have appeared to influence the work reported in this paper.

Acknowledgments

We are grateful to Hitoshi Kanno (Tohoku University) and Toyoaki Ito (Niigata Agro-Food University) for providing samples of non-allophanic Andisols. This study was funded in part by KAKENHI provided by Ministry of Education, Culture, Sports, Science and Technology, Japan (Grant number: 15H04467, 26660051). The XANES spectroscopy experiments were conducted at BL6N1 in Aichi Synchrotron Radiation Center, Aichi Science & Technology Foundation, Japan.

Appendix A. Supplementary data

Supplementary data to this article can be found online at https://doi.org/10.1016/j.geoderma.2021.115080.

References

Asano, M., Wagai, R., 2014. Evidence of aggregate hierarchy at micro- to submicron scales in an allophanic Andisol. Geoderma 216, 62–74.
W.T. Baisden R. Amundson A.C. Cook D.L. Brenner Turnover and storage of C and N in five density fractions from California annual grassland surface soils Global Biogeochemical Cycles 16 4 2002 64–61-64-16.
Bascomb, C.L., 1968. Distributin of pyrophosphate-extractable iron and organic carbon in soils of various groups. J. Soil Sci. 19 (2), 251–268.
Borggaard, O.K., 1992. Dissolution of poorly crystalline iron oxides in soils by EDTA and oxalate. Zeitschrift für Pflanzenernährung und Bodenkunde 155 (5), 431–436.
Borie, F., Zunino, H., Martínez, L., 1989. Macromolecule-P associations and inositol phosphates in some chilean volcanic soils of temperate regions. Commun. Soil Sci. Plant Anal. 20 (17–18), 1881–1894.
Cade-Menun, B., Liu, C.W., 2014. Solution phosphorus-31 nuclear magnetic resonance spectroscopy of soils from 2005 to 2013: a review of sample preparation and experimental parameters. Soil Sci. Soc. Am. J. 78 (1), 19–37.
Condron, L.M., Newman, S., 2011. Revisiting the fundamentals of phosphorus fractionation of sediments and soils. J. Soils Sediments 11 (5), 830–840.
Cornell, R.M., Schwertmann, U., 2006. The Iron Oxides: Structure, Properties, Reactions, Occurrences and Uses. John Wiley & Sons.
Coward, E.K., Ohno, T., Plante, A.F., 2018. Adsorption and molecular fractionation of dissolved organic matter on iron-bearing mineral matrices of varying crystallinity. Environ. Sci. Technol. 52 (3), 1036–1044.
Crow, S.E., Reeves, M., Schubert, O.S., Sierra, C.A., 2015. Optimization of method to quantify soil organic matter dynamics and carbon sequestration potential in volcanic ash soils. Biogeochemistry 123 (1), 27–47.
De Groot, C.J., Golterman, H.L., 1993. On the presence of organic phosphate in some Camargue sediments: evidence for the importance of phytate. Hydrobiologia 252 (1), 117–126.
Doolette, A.L., Smernik, R.J., Dougherty, W.J., 2011. Overestimation of the importance of phytate in NaOH–EDTA soil extracts as assessed by ^{31}P NMR analyses. Org Geochem. 42 (8), 955–964.
Gerke, J., 2010. Humic (organic matter)-Al(Fe)-phosphate complexes: an underestimated phosphate form in soils and source of plant-available phosphate. Soil Sci. 175 (9), 417–425.
Giaveno, C., Celi, L., Richardson, A.E., Simpson, R.J., Barberis, E., 2010. Interaction of phytases with minerals and availability of substrate affect the hydrolysis of inositol phosphates. Soil Biol. Biochem. 42 (3), 491–498.
Giesler, R., Andersson, T., Lövgren, L., Persson, P., 2005. Phosphate sorption in aluminum- and iron-rich humus soils. Soil Sci. Soc. Am. J. 69 (1), 77–86.
Giguet-Covex, C., Poulenard, J., Chalmin, E., Arnaud, F., Rivard, C., Jenny, J.P., Dorioz, J.M., 2013. XANES spectroscopy as a tool to trace phosphorus transformation during soil genesis and mountain ecosystem development from lake sediments. Geochim. Cosmochim. Acta 118, 129–147.
Gu, C., Dam, T., Hart, S.C., Turner, B.L., Chadwick, O.A., Berhe, A.A., Hu, Y., Zhu, M., 2020. Quantifying uncertainties in sequential chemical extraction of soil phosphorus using XANES spectroscopy. Environ. Sci. Technol. 54 (4), 2257–2267.
Gunjigake, N., Wada, K., 1981. Effects of phosphorus concentration and pH on phosphate retention by active aluminum and iron of Ando soils. Soil Sci. 132 (5), 347–352.
Hashimoto, Y., Kang, J., Matsuyama, N., Saigusa, M., 2012. Path analysis of phosphorus retention capacity in allophanic and non-allophanic Andisols. Soil Sci. Soc. Am. J. 76 (2), 441–448.
Hashimoto, Y., Takamoto, A., Kikkawa, R., Murakami, K., Yamaguchi, N., 2014. Formations of hydroxyapatite and inositol hexakisphosphate in poultry litter during the composting period: sequential fractionation, P K-edge XANES and solution ^{31}P NMR investigations. Environ. Sci. Technol. 48 (10), 5486–5492.
Hedley, M.J., Stewart, J.W.B., Chauhan, B.S., 1982. Changes in inorganic and organic soil phosphorus fractions induced by cultivation practices and by laboratory incubations. Soil Sci. Soc. Am. J. 46 (5), 970–976.
Hesterberg, D., 2010. Chapter 11 - Macroscale Chemical Properties and X-Ray Absorption Spectroscopy of Soil Phosphorus. In: Singh, B., Gräfe, M. (Eds.), Developments in Soil Science. Elsevier, pp. 313–356.
Hesterberg, D., Zhou, W., Hutchison, K.J., Beauchemin, S., Sayers, D.E., 1999. XAFS study of adsorbed and mineral forms of phosphate. J. Synchrotron Radiat. 6 (3), 636–638.
Hiradate, S., Uchida, N., 2004. Effects of soil organic matter on pH-dependent phosphate sorption by soils. Soil Sci. Plant Nutr. 50 (5), 665–675.
Hou, E., Chen, C., McGroddy, M.E., Wen, D., 2012. Nutrient limitation on ecosystem productivity and processes of mature and old-growth subtropical forests in China. PLoS One 7 (12), e52071.

Ito, T., Saigusa, M., 1996. Characteristics of nonallophanic Andisols at Tohoku University Farm. Bull. Exp. Farm Tohoku Univ. 12, 91–103.
Jones, E., Singh, B., 2014. Organo-mineral interactions in contrasting soils under natural vegetation. Front. Environ. Sci. 2 (2).
Kaiser, K., Guggenberger, G., 2007. Distribution of hydrous aluminium and iron over density fractions depends on organic matter load and ultrasonic dispersion. Geoderma 140 (1–2), 140–146.
Kaiser, K., Guggenberger, G., Zech, W., 1996. Sorption of DOM and DOM fractions to forest soils. Geoderma 74 (3), 281–303.
Loveland, P.J., Digby, P., 1984. The extraction of Fe and Al by 0.1 M pyrophosphate solutions: A comparison of some techniques. J. Soil Sci. 35 (2), 243–250.
Martin, M., Celi, L., Barberis, E., 1999. Determination of low concentrations of organic phosphorus in soil solution. Commun. Soil Sci. Plant Anal. 30 (13–14), 1909–1917.
Martin, M., Celi, L., Barberis, E., 2004. Desorption and plant availability of myo-inositol hexaphosphate adsorbed on goethite. Soil Sci. 169 (2), 115–124.
Matsuyama, N., 1994. Classification of Japanese Andosols Based on Poorlycrystalline Minerals and Soil Management Schemes. Ph.D. diss. (In Japanese) Tohoku Univ, Miyagi, Japan.
Mayer, L.M., Schick, L.L., Hardy, K.R., Wagai, R., McCarthy, J., 2004. Organic matter in small mesopores in sediments and soils. Geochim. Cosmochim. Acta 68 (19), 3863–3872.
McLaren, T.I., Smernik, R.J., McLaughlin, M.J., McBeath, T.M., Kirby, J.K., Simpson, R. J., Guppy, C.N., Doolette, A.L., Richardson, A.E., 2015. Complex forms of soil organic phosphorus–A major component of soil phosphorus. Environ. Sci. Technol. 49 (22), 13238–13245.
Mori, T., Wachrinrat, C., Staporn, D., Meunpong, P., Suebsai, W., Matsubara, K., Boonsri, K., Lumban, W., Kuawong, M., Phukdee, T., Srifai, J., Boonman, K., 2017. Effects of phosphorus addition on nitrogen cycle and fluxes of N_2O and CH_4 in tropical tree plantation soils in Thailand. Agric. Nat. Resour. 51 (2), 91–95.
Nanzyo, M., Dahlgren, R., Shoji, S., 1993. Chapter 6 Chemical characteristics of volcanic ash soils. In: Shoji, S., Nanzyo, M., Dahlgren, R. (Eds.), Developments in Soil Science. Elsevier, pp. 145–187.
Parfitt, R.L., Childs, C.W., 1988. Estimation of forms of Fe and Al- a review, and analysis of contrasting soils by dissolution and Mossbauer methods. Aust. J. Soil Res. 26 (1), 121–144.
Percival, H.J., Parfitt, R.L., Scott, N.A., 2000. Factors Controlling Soil Carbon Levels in New Zealand Grasslands Is Clay Content Important? Soil Sci. Soc. Am. J. 64 (5), 1623–1630.
Pierzynski, G.M., Logan, T.J., Traina, S.J., Bigham, J.M., 1990. Phosphorus chemistry and mineralogy in excessively fertilized soils: Quantitative-analysis of phosphorus-rich particles. Soil Sci. Soc. Am. J. 54 (6), 1576–1583.
Prietzel, J., Harrington, G., Hausler, W., Heister, K., Werner, F., Klysubun, W., 2016. Reference spectra of important adsorbed organic and inorganic phosphate binding forms for soil P speciation using synchrotron-based K-edge XANES spectroscopy. J. Synchrotron Radiat. 23 (2), 532–544.
Ravel, B., Newville, M., 2005. ATHENA, ARTEMIS, HEPHAESTUS: data analysis for X-ray absorption spectroscopy using IFEFFIT. J. Synchrotron Radiat. 12 (4), 537–541.
Rennert, T., 2019. Wet-chemical extractions to characterise pedogenic Al and Fe species – A critical review. Soil Res. 57 (1), 1–16.
Saigusa, M., Toma, M., Abe, T., 1994. Effects of phosphogypsum application in topsoil on amelioration of subsoil acidity of nonallophanic Andosols. J. Japan. Grassl. Sci 39 (4), 397–404.
Schubert, S., Steffens, D., Ashraf, I., 2020. Is occluded phosphate plant-available? J. Plant Nutr. Soil Sci. 183 (3), 338–344.
Schuppli, P.A., Ross, G.J., McKeague, J.A., 1983. The Effective removal of suspended materials from pyrophosphate extracts of soils from tropical and temperate regions. Soil Sci. Soc. Am. J. 47 (5), 1026–1032.
Shang, C., Stewart, J.W.B., Huang, P.M., 1992. pH effect on kinetics of adsorption of organic and inorganic phosphates by short-range ordered aluminum and iron precipitates. Geoderma 53 (1), 1–14.
Shoji, S., Dahlgren, R., Nanzyo, M., 1993. Volcanic Ash Soils, Genesis, Properties, and Utilization. Elsevier, Amsterdam.
Shoji, S., Fujiwara, Y., 1984. Active aluminum and iron in the humus horizons of Andosols from northeastern Japan: their forms, properties, and significance in clay weathering. Soil Sci. 137 (4), 216–226.
Six, J., Guggenberger, G., Paustian, K., Haumaier, L., Elliott, E.T., Zech, W., 2001. Sources and composition of soil organic matter fractions between and within soil aggregates. Eur. J. Soil Sci. 52 (4), 607–618.
Smeck, N.E., 1985. Phosphorus dynamics in soils and landscapes. Geoderma 36 (3), 185–199.
Sollins, P., Glassman, C., Paul, E., Swanston, C., Lajtha, K., Heil, J., Elliott, E., 1999. In: Soil Carbon and Nitrogen Pools and Fractions, Standard Soil Methods for Long-term Ecological Research. Oxford University Press, Oxford, pp. 89–105.
Sollins, P., Kramer, M.G., Swanston, C., Lajtha, K., Filley, T., Aufdenkampe, A.K., Wagai, R., Bowden, R.D., 2009. Sequential density fractionation across soils of contrasting mineralogy: Evidence for both microbial- and mineral-controlled soil organic matter stabilization. Biogeochemistry 96 (1), 209–231.
Sollins, P., Swanston, C., Kleber, M., Filley, T., Kramer, M., Crow, S., Caldwell, B.A., Lajtha, K., Bowden, R., 2006. Organic C and N stabilization in a forest soil: Evidence from sequential density fractionation. Soil Biol. Biochem. 38 (11), 3313–3324.
Sparks, D.L., Page, A., P., H., Loeppert, R., Soltanpour, P., Tabatabai, M., Johnston, C., Sumner, M. 1996. Methods of soil analysis. Part 3-Chemical methods. Soil Science Society of America Inc.
Takahashi, T., Dahlgren, R.A., 2016. Nature, properties and function of aluminum–humus complexes in volcanic soils. Geoderma 263, 110–121.
Takamoto, A., Hashimoto, Y., 2014. Assessment of hedley's sequential extraction method for phosphorus forms in biosolids using P K-edge X-ray absorption near-edge Structure Spectroscopy. Chem. Lett. 43 (11), 1696–1697.
Turchenek, L.W., Oades, J.M., 1979. Fractionation of organo-mineral complexes by sedimentation and density techniques. Geoderma 21 (4), 311–343.
Turner, B.L., Laliberté, E., 2015. Soil development and nutrient availability along a 2 million-year coastal dune chronosequence under species-rich Mediterranean Shrubland in southwestern Australia. Ecosystems 18 (2), 287–309.
Turner, B.L., Mahieu, N., Condron, L.M., 2003. Phosphorus-31 nuclear magnetic resonance spectral assignments of phosphorus compounds in soil NaOH-EDTA extracts. Soil Sci. Soc. Am. J. 67 (2), 497–510.
Turner, B.L., Richardson, A.E., 2004. Identification of scyllo-inositol phosphates in soil by solution phosphorus-31 nuclear magnetic resonance spectroscopy. Soil Sci. Soc. Am. J. 68 (3), 802–808.
Velásquez, G., Ngo, P.-T., Rumpel, C., Calabi-Floody, M., Redel, Y., Turner, B.L., Condron, L.M., Mora, M.d.l.L. 2016. Chemical nature of residual phosphorus in Andisols. Geoderma 271, 27–31.
Wagai, R., Kajiura, M., Asano, M., 2020. Iron and aluminum association with microbially processed organic matter via meso-density aggregate formation across soils: Organo-metallic glue hypothesis. Soil Discuss. 2020, 1–42.
Wagai, R., Kajiura, M., Uchida, M., Asano, M., 2018. Distinctive Roles of Two Aggregate Binding Agents in Allophanic Andisols: Young carbon and poorly-crystalline metal phases with old carbon. Soil Syst. 2 (2), 29.
Wagai, R., Mayer, L.M., Kitayama, K., Knicker, H., 2008. Climate and parent material controls on organic matter storage in surface soils: A three-pool, density-separation approach. Geoderma 147 (1), 23–33.
Wagai, R., Mayer, L.M., Kitayama, K., Shirato, Y., 2013. Association of organic matter with iron and aluminum across a range of soils determined via selective dissolution techniques coupled with dissolved nitrogen analysis. Biogeochemistry 112 (1), 95–109.
Wang, Y.P., Law, R.M., Pak, B., 2010. A global model of carbon, nitrogen and phosphorus cycles for the terrestrial biosphere. Biogeosciences 7 (7), 2261–2282.
Werner, F., Mueller, C.W., Thieme, J., Gianoncelli, A., Rivard, C., Hoschen, C., Prietzel, J., 2017. Micro-scale heterogeneity of soil phosphorus depends on soil substrate and depth. Sci. Rep. 7.
Yamamoto, K., Hashimoto, Y., 2017. Chemical species of phosphorus and zinc in water-dispersible colloids from swine manure compost. J. Environ. Qual. 46 (2), 461–465.
Yamamoto, K., Hashimoto, Y., Kang, J., Kobayashi, K., 2018. Speciation of phosphorus zinc and copper in soil and water-dispersible colloid affected by a long-term application of swine manure compost. Environ. Sci. Technol. 52 (22), 13270–13278.